The EMBO Journal vol.14 no.10 pp.2269–2280, 1995

39 kDa receptor-associated protein is an ER resident protein and molecular chaperone for LDL receptor-related protein

Guojun Bu[1], Hans J.Geuze[2], Ger J.Strous[2] and Alan L.Schwartz

Departments of Pediatrics and Molecular Biology and Pharmacology, Washington University School of Medicine, St Louis, MO 63110, USA and [2]Department of Cell Biology, University of Utrecht, 3584 CH Utrecht, The Netherlands

[1]Corresponding author

The low density lipoprotein receptor-related protein (LRP) is a multifunctional endocytic receptor with the ability to bind and endocytose several structurally and functionally distinct ligands. A 39 kDa receptor-associated protein (RAP) inhibits all ligand interactions with LRP *in vitro*. In the present study, we demonstrate that RAP is an endoplasmic reticulum (ER) resident protein. The tetrapepetide sequence HNEL at the C-terminus of RAP is both necessary and sufficient for RAP retention within the ER. Metabolic labeling combined with cross-linking studies shows that RAP interacts with LRP *in vivo*. Pulse–chase analysis reveals that this association is transient early in the secretory pathway and coincides with LRP aggregation and reduced ligand binding activity. Both internal triplicated LRP binding domains on RAP and multiple RAP binding domains on LRP appear to contribute to the aggregation of LRP and RAP. Dissociation of RAP from LRP results from the lower pH encountered later in the secretory pathway and correlates with an increase in LRP ligand binding activity. Taken together, our results thus suggest that RAP functions intracellularly as a molecular chaperone for LRP and regulates its ligand binding activity along the secretory pathway.

Key words: ER retention/LRP/molecular chaperone/RAP/secretory pathway

Introduction

The low density lipoprotein (LDL) receptor-related protein (LRP) is a member of the LDL receptor gene family which includes the well characterized LDL receptor (Yamamoto *et al.*, 1984), a kidney membrane protein gp330 (Raychowdhury *et al.*, 1989) and a recently identified very low density lipoprotein (VLDL) receptor (Takakashi *et al.*, 1992). LRP is an endocytic receptor unique both for its large size (600 kDa, see Herz *et al.*, 1988) and its ability to bind and endocytose several structurally and functionally distinct ligands (see Krieger and Herz, 1994). Ligands of LRP include α_2-macroglobulin–protease complexes (α_2M^*, Kristensen *et al.*, 1990; Strickland *et al.*, 1990); tissue-type plasminogen activator (t-PA) either in its free form (Bu *et al.*, 1992) or complexed with plasminogen activator inhibitor type-1 (PAI-1) (Orth *et al.*, 1992; Bu *et al.*, 1993); urokinase plasminogen activator (u-PA) and PAI-1 complexes (Nykjaer *et al.*, 1992; Herz *et al.*, 1992); β-migrating VLDL (β-VLDL) complexed with either apolipoprotein E (apoE, Beisiegel *et al.*, 1989; Kowal *et al.*, 1989) or lipoprotein lipase (Willnow *et al.*, 1992; Nykjaer *et al.*, 1993); *Pseudomonas* exotoxin A (Kounnas *et al.*, 1992); lactoferrin (Willnow *et al.*, 1992); and tissue factor pathway inhibitor (TFPI, Warshawsky *et al.*, 1994). The diversity of these ligands implies that LRP may function as a specific endocytic receptor in a variety of distinct physiological processes.

Most ligands bind to LRP at distinct sites and do not compete with one another for binding (Bu *et al.*, 1992; Willnow *et al.*, 1992). This abundance of distinct ligand binding sites may relate to the large size and repeated sequence of LRP. The extracellular portion of LRP contains four ligand binding domains each resembling the apoE binding domain of the LDL receptor (Herz *et al.*, 1988). A unique ligand, termed LRP receptor-associated protein (RAP), inhibits all known ligand interactions with LRP (Herz *et al.*, 1991; Bu *et al.*, 1992; Warshawsky *et al.*, 1993). RAP, also known as the 39 kDa protein owing to its molecular size, co-purifies with LRP and binds to LRP with high affinity (Strickland *et al.*, 1990, 1991; Herz *et al.*, 1991; Iadonato *et al.*, 1993). The mechanism(s) by which RAP inhibits the binding and/or uptake of LRP ligands is not clear. LRP contains approximately six times as many binding sites for RAP compared with t-PA (Iadonato *et al.*, 1993) and the binding of at least two of the LRP ligands, α_2M^* and t-PA, is differentially inhibited by RAP (Warshawsky *et al.*, 1993). These studies, using truncated RAP constructs, indicate that the N-terminal domain of RAP inhibits both α_2M^* and t-PA binding, whereas the C-terminal domain inhibits only t-PA binding. These data suggest that each independent ligand binding site on LRP may also bind RAP, and that each of these RAP binding sites bears distinct binding determinants on the RAP molecule.

Despite the presence of a putative signal peptide (Strickland *et al.*, 1991), RAP has not been detected extracellularly. The inability to detect extracellular RAP in cell culture media or circulating plasma may be due to rapid flux, as RAP is avidly taken up and degraded via LRP (Iadonato *et al.*, 1993). Using colloidal gold immunoelectron microscopy and U87 cells which express abundant LRP and RAP, RAP was localized most abundantly within the endoplasmic reticulum (ER, 70%) and Golgi compartments (24%) with only 2% of the total RAP found on the cell surface and 4% in the endosomes (Bu *et al.*, 1994a). These observations suggest that the normal physiological function of RAP may be intracellular. In the current study, we demonstrate that the C-terminal tetrapeptide, HNEL, is responsible for the ER localization and retention of RAP. ER retained RAP functions as a

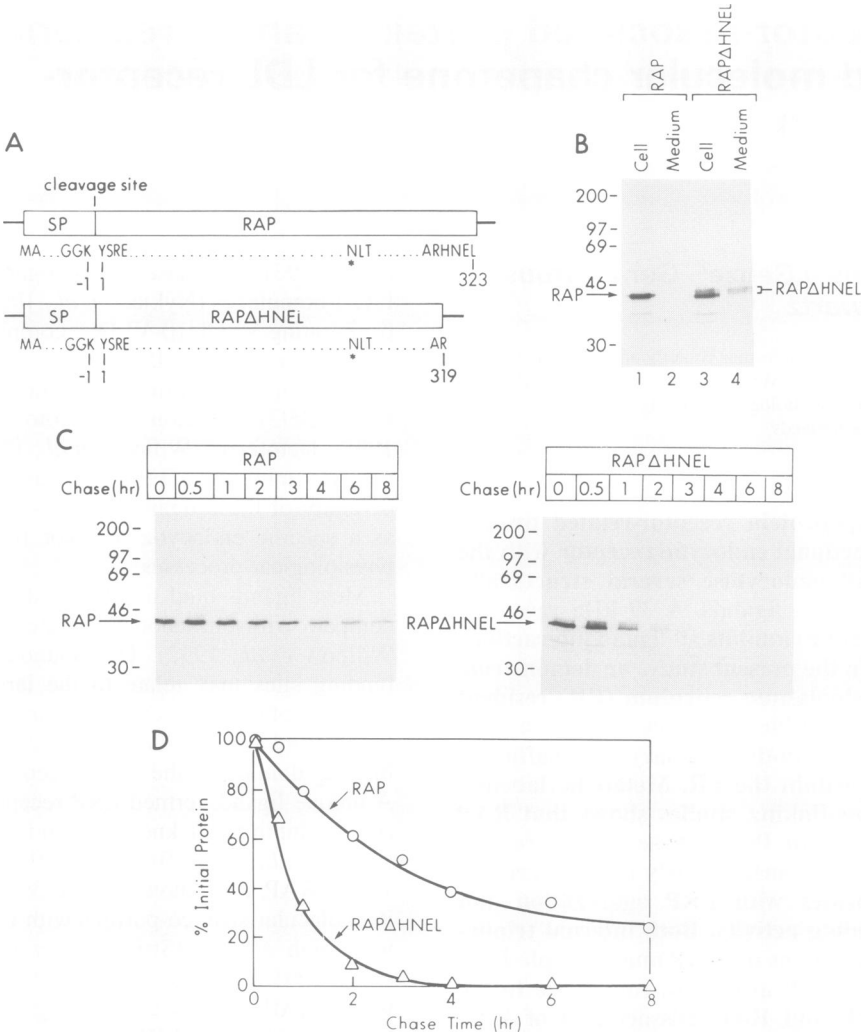

Fig. 1. Deletion of HNEL sequence from RAP accelerated its secretion and shortened its intracellular half-life. (**A**) Schematic representation of the two plasmids containing cDNAs of either full-length RAP (RAP) or RAP with the last four amino acids, HNEL, deleted (RAPΔHNEL). The putative *N*-linked glycosylation site is indicated with *. SP represents RAP signal peptide and the thicker lines at each end of the cDNA constructs represent the vector sequence of pcDNA3. (**B**) U87 cells stably transfected with either RAP (G16 cells) or RAPΔHNEL (H1 cells) were metabolically labeled with [^{35}S]methionine for 1 h. Cell lysates and the overlying media were then immunoprecipitated with anti-RAP antibody. Samples were analyzed on 10% SDS–polyacrylamide gel. The positions of RAP and RAPΔHNEL are labeled. The molecular weight standards in this figure and the following figures are given on the left in kDa. (**C**) U87 cells transfected with either RAP (G16 cells) or RAPΔHNEL (H1 cells) were pulse-labeled with [^{35}S]methionine for 30 min, and chased with serum-containing medium for various periods of time as indicated. After each chase, cell lysate was immunoprecipitated with anti-RAP antibody and analyzed on 10% SDS–polyacrylamide gels. The positions of RAP and RAPΔHNEL are labeled. (**D**) The amount of RAP from each chase was measured by densitometry from the fluorograghs shown in (C) and plotted against chase time.

molecular chaperone for LRP by transiently interacting with LRP and maintaining LRP in an inactive ligand binding state. As RAP dissociates from LRP in response to the low pH within the Golgi, LRP becomes active as it travels to the cell surface.

Results

HNEL sequence at the C-terminus of RAP is required for ER retention

To investigate whether the HNEL sequence at the C-terminus of RAP serves as an ER retention signal, we generated two cDNA constructs by reverse transcriptase-polymerase chain reaction (RT-PCR): full-length RAP and RAP with the HNEL sequence deleted (designated as RAP and RAPΔHNEL, respectively, see Figure 1A). The two cDNA constructs were subcloned into a mammalian expression vector pcDNA3 and stably transfected into U87 cells. Five transfected clones were selected for each construct. When the expression of RAP from the transfected cell lines was analyzed by Western blotting using anti-RAP antibody, we found that each clone expressed ~20–50 times more RAP than untransfected U87 cells (data not shown). One line from RAP-transfected (G16) and one line from RAPΔHNEL-transfected (H1) cells were used for further analysis (see below).

To investigate whether overexpression of RAP resulted in its secretion, we labeled G16 and H1 cells with [^{35}S]methionine for 1 h and immunoprecipitated the cell lysates and the overlying media with anti-RAP antibody (Figure 1B). No RAP was detected in the media from full-length RAP-transfected G16 cells (lane 2), whereas RAP was readily detected from the media of RAPΔHNEL-transfected H1 cells (lane 4). The secreted RAPΔHNEL

migrated identically to a minor upper band seen in cell lysates (lane 3). This upper band resulted from complex carbohydrate modification, as discussed below. After quantification of the band intensity of RAPΔHNEL from both medium and cells, we found that, at steady state after 1 h of continuous labeling, ~15% total radiolabeled RAPΔHNEL associated with the medium and 85% associated with the cells. These results indicated that deletion of the HNEL sequence accelerated RAP secretion and is consistent with the participation of HNEL in the ER retention of RAP. When G16 cells were labeled for 4 h, RAP secretion was observed with G16 cells, although to a lesser degree than with the H1 cells (data not shown).

To compare directly the intracellular half-life of RAP and RAPΔHNEL, we performed pulse–chase analysis on both G16 and H1 cells. Cells were pulse-labeled with [^{35}S]methionine for 30 min and chased for different periods of time up to 8 h. As seen in Figure 1C, RAPΔHNEL disappeared rapidly from the cell compared with full-length RAP. When band intensities were measured by densitometry and plotted against chase time (Figure 1D), we found that the half-life of intracellular RAP decreased from ~3 h for full-length RAP to ~40 min for RAPΔHNEL. These results indicated that deletion of the HNEL sequence shortened its intracellular half-life. Owing to the overexpression of RAP, the intracellular half-life in transfected cells is presumably much shorter than that found under normal conditions. As the RAP sequence lacks cysteine and contains only one methionine residue, and since untransfected U87 cells express a much lower amount of RAP, attempts to determine the half-life of RAP in untransfected cells have been inconclusive (data not shown). However, as the rat sequence contains three methionines (Pietromonaco *et al.*, 1990), we have determined the half-life of RAP in two rat cell lines and found that it ranges from 13 to 18 h (Warshawsky and Schwartz, unpublished results).

To compare the subcellular distribution of full-length RAP and RAPΔHNEL, we immunolabeled stably transfected G16 and H1 cells with anti-RAP antibody followed by colloidal gold probes (Figure 2). As illustrated in Figure 2A and described earlier (Bu *et al.*, 1994a), RAP was localized mainly within the rough ER (RER) and Golgi complex, with some immunolabeling in endosomes marked with endocytosed bovine serum albumin (BSA)–gold particles. Cross-sections through the Golgi complexes in G16 cells clearly showed that RAP is confined predominantly to the *cis*-elements of the Golgi complex, including one or two *cis*-cisternae and the intermediate compartment. The latter was identified by double-labeling with anti-p53 (Schweizer *et al.*, 1988; data not shown). Only scarce RAP labeling was seen at the *trans*-Golgi cisternae and the *trans*-Golgi network (TGN) as noted by characteristic coated buds and vesicles (Figure 2A). RAPΔHNEL also localized to the RER but, in contrast to RAP, was found throughout the Golgi stacks of cisternae (Figure 2B, C), and within the electron-dense vesicles in the *trans*-Golgi area (Figure 2B). In addition, RAPΔHNEL was present more abundantly than RAP within endosomes pre-loaded with BSA–gold particles. These results are consistent with the notion that deletion of the HNEL sequence from RAP abrogates its ER retention, allows the protein to exit the ER, transit the secretory pathway, interact with endocytic receptor(s) on the cell surface (e.g. LRP) and be endocytosed.

ER-retained RAP includes a population of endo H-resistant species which lacks complex carbohydrate modification

The above pulse–chase experiments showed that while RAPΔHNEL migrated at an apparently increased molecular mass soon after its biosynthesis, the full-length RAP did not, even after a prolonged period of chase (Figure 1C). To investigate whether all the full-length RAP are identical in their carbohydrate modifications, we determined their sensitivity to endo H. RAP-transfected G16 cells or RAPΔHNEL-transfected H1 cells were continuously labeled with [^{35}S]methionine for 4 h and cell lysates were immunoprecipitated with anti-RAP antibody. When the protein from RAP-transfected cells was subjected to endo H digestion, ~35% of the total labeled protein was found to be resistant to endo H digestion (Figure 3A, lane 2, band a) with the remaining 65% sensitive (lane 2, band b). Control experiments showed that this was not a result of incomplete endo H digestion since an identical percentage of endo H-resistant RAP was observed with increasing amounts of endo H (data not shown). The endo H-sensitive RAP presumably represents the protein within the ER, whereas the endo H-resistant RAP must have exited the ER and crossed the medial-Golgi compartment (Kornfeld and Kornfeld, 1985). The same band from RAPΔHNEL-transfected cells (lane 3, band a) exhibited complete endo H sensitivity (from band a to band b). This suggests that, following the deletion of the HNEL sequence, RAP transiently passes through these compartments en route to the cell surface without significant retention. To study the kinetics of the generation of the endo H-resistant form, G16 cells were pulse labeled for 30 min and chased for increasing periods of time up to 8 h. Initially (Figure 3B, lane 1, 0 chase), all the newly synthesized RAP exhibited endo H sensitivity. With increasing chase time, the endo H-sensitive species decreased with a concomitant increase of the endo H-resistant species. At the end of the chase (8 h), >80% of the total RAP protein became endo H resistant. These results indicate that newly synthesized RAP slowly trafficks to the medial-Golgi compartment where endo H-resistant modification occurs (Kornfeld and Kornfeld, 1985; Schwaninger *et al.*, 1991). We also performed pulse–chase labeling and endo H digestion for RAPΔHNEL in H1 cells. The pattern of endo H sensitivity is identical for all the chase periods analyzed, and is similar to that shown in Figure 3A, right panel.

HNEL resembles the KDEL sequence and is sufficient for ER retention

Having demonstrated that the HNEL sequence of RAP is required for ER retention, we then investigated whether the HNEL sequence can function similarly to the KDEL sequence and whether it is sufficient for retention of a normally secreted protein. We chose human growth hormone (GH) as a test protein since U87 cells do not express endogenous GH. Three cDNA constructs were generated with PCR and subcloned into the expression vector pcDNA3. These include: (i) wild-type GH; (ii) GH with the KDEL sequence attached to the C-terminus; and

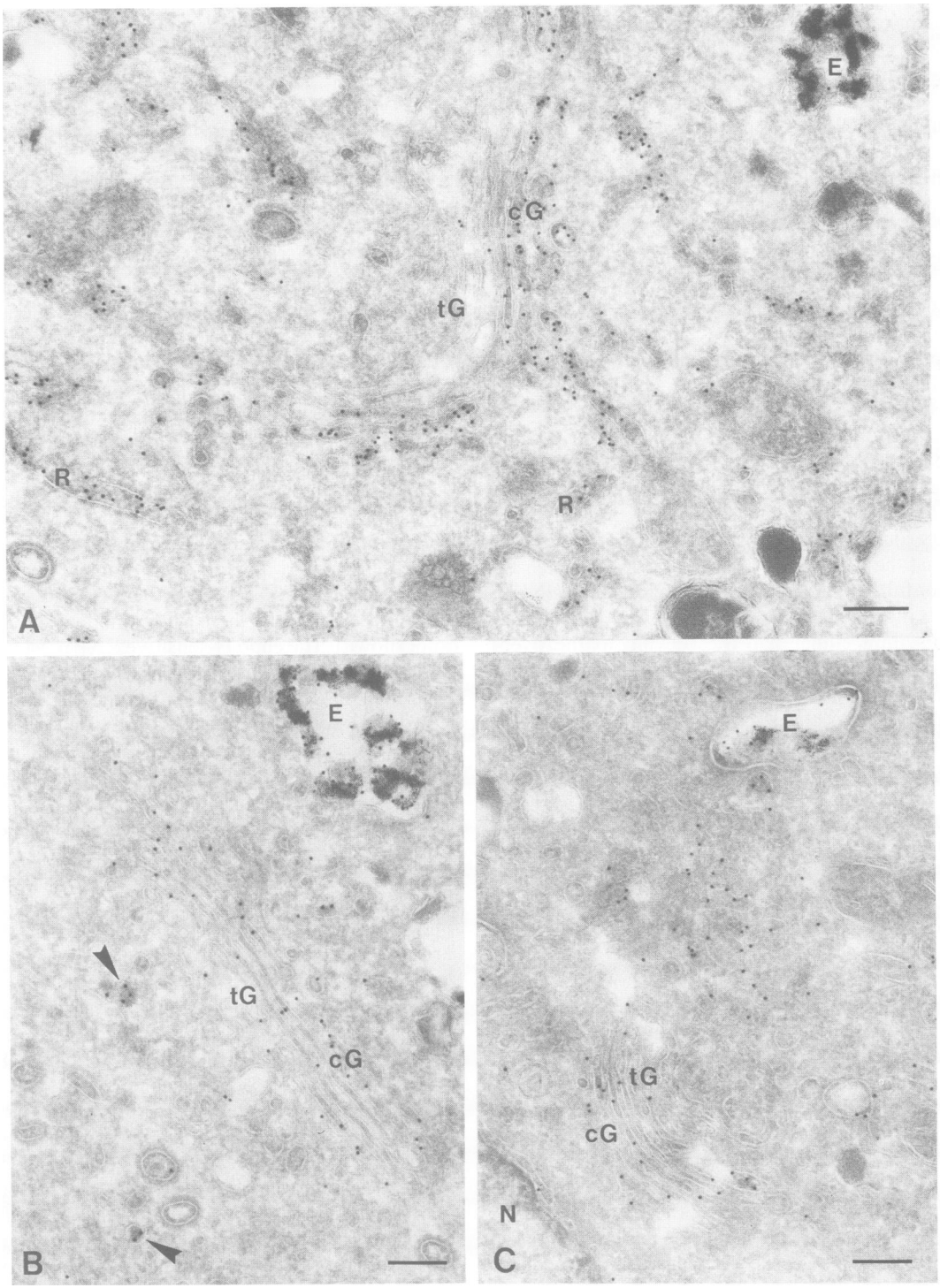

Fig. 2. Immunogold electron microscopy localization of RAP and RAPΔHNEL. Immunoelectron micrographs of ultrathin cryosections from stably transfected G16 and H1 cells labeled with 10 nm gold particles for the demonstration of RAP (A) and RAPΔHNEL (B and C). Prior to fixation, the cells were allowed to endocytose 5 nm BSA–gold particles for 1 h. Bars represent 200 nm. (**A**) G16 cells showing RAP present in the rough endoplasmic reticulum (R) and in *cis*-Golgi elements (cG). The *trans*-Golgi elements (tG) are largely devoid of detectable RAP. Some RAP was found in endosomes marked with endocytosed BSA–gold particles (E). (**B** and **C**) H1 cells showing RAPΔHNEL present throughout the Golgi stacks, in endosomes (E) containing BSA–gold particles and in electron-dense vesicles (arrowhead) in the *trans*-Golgi area. N, nucleus.

(iii) GH with the HNEL sequence attached to the C-terminus. These three constructs together with vector alone were then transiently transfected into U87 cells and the kinetics of GH secretion were studied. Transiently transfected cells were pulse-labeled with [^{35}S]methionine for 30 min and chased for 60 min (Figure 4A). At 30 min of chase, half of the overlying medium from each transfection was removed for analysis of GH secretion. At 60 min the remaining media and the cell lysates were analyzed. The intensity of each band was quantitated and plotted for comparison (Figure 4B). As seen in the figure, >80% of the wild-type GH was secreted at the end of

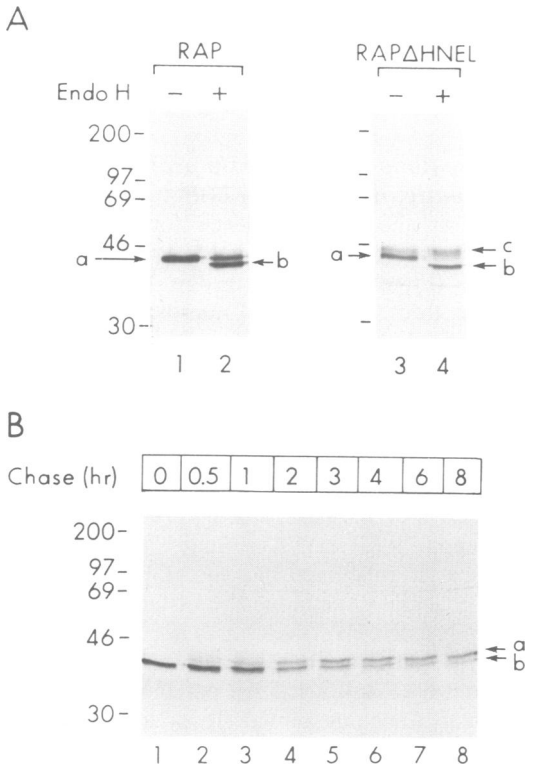

Fig. 3. Intracellular RAP includes an endo H-resistant species which lacks complex carbohydrate modification. (**A**) U87 cells stably transfected with either RAP (G16 cells) or RAPΔHNEL (H1 cells) were metabolically labeled with [^{35}S]methionine for 4 h and immunoprecipitated with anti-RAP antibody. Cell lysates were incubated in the absence or presence of endo H and analyzed on 10% SDS–polyacrylamide gel. The position labeled with 'a' represents RAP with simple carbohydrate modification (includes both endo H-sensitive and -resistant species), whereas the position labeled with 'b' indicates endo H-sensitive RAP or RAPΔHNEL which had simple carbohydrate modification removed by endo H. The position 'c' represents the species which contains complex carbohydrate modification (endo H-resistant). (**B**) U87 cells stably transfected with RAP (G16 cells) were pulse-labeled and chased as in Figure 1C. After each chase, cell lysates were immunoprecipitated with anti-RAP antibody and subjected to endo H digestion. The position labeled 'a' represents endo H-resistant RAP, whereas the position labeled 'b' indicates endo H-sensitive RAP with simple carbohydrate modification removed by endo H. All samples were analyzed on 10% SDS–polyacrylamide gels.

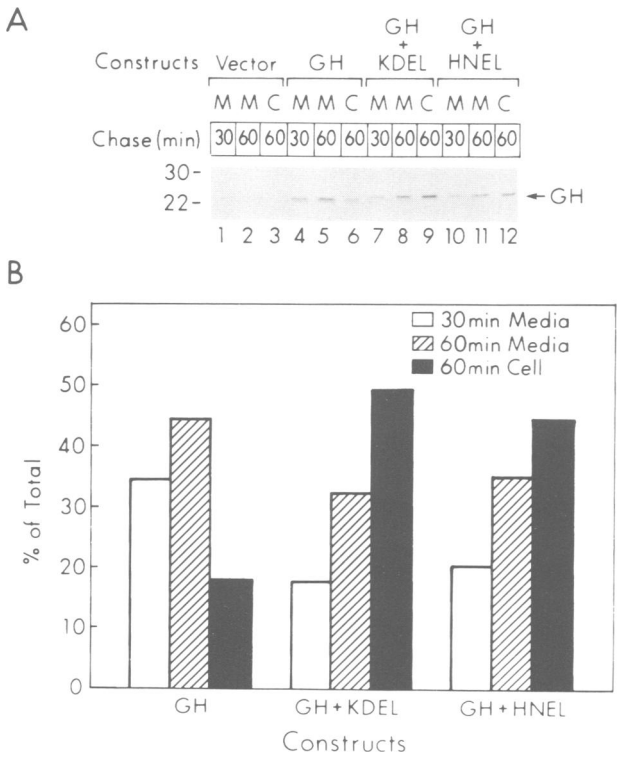

Fig. 4. Retention of GH by KDEL and HNEL. (**A**) U87 cells were transiently transfected with the following plasmids: pcDNA3 (vector), pcDNA3 containing wild-type GH (GH), pcDNA3 containing GH with KDEL attached to the C-terminus (GH+KDEL) or pcDNA3 containing GH with HNEL attached to the C-terminus (GH+HNEL). For each transfection, cells were pulse-labeled with [^{35}S]methionine for 30 min. After 30 min chase, half of the medium was removed from each transfection. After 60 min chase, the remaining medium and cell lysate from each transfection were harvested. Media and cell lysates were then immunoprecipitated with anti-GH antibody before they were analyzed on 15% SDS–polyacrylamide gel. Proteins from GH+KDEL or GH+HNEL transfections migrated slightly slower on the gel than that of wild-type GH transfection, reflecting their larger sizes as a result of addition of amino acids. (**B**) The amount of GH from each sample was measured by densitometry from the fluorogragh in (A). One hundred percent represents the total radiolabeling from 30 min medium, 60 min medium and 60 min cell lysates.

60 min chase, whereas almost 50% of GH containing either KDEL or HNEL remained within the cell. It is unlikely that the addition of KDEL and HNEL tetrapeptides at the C-terminus of GH would cause significant misfolding of the protein. Therefore, the retention of GH+KDEL and GH+HNEL must have resulted from interactions between these tetrapeptides and ER retention receptor(s). The incomplete retention by either the KDEL or HNEL sequence is presumably due to the overexpression of the proteins and saturation of the retention system(s).

RAP interacts with LRP inside the cell

To examine the function of RAP within the ER, we performed chemical cross-linking experiments *in vivo* on U87 cells (Figure 5A). Cells were metabolically labeled with [^{35}S]cysteine for 5 h. Intracellular proteins were cross-linked either with the membrane-impermeable cross-linker DTSSP following permeablization of cells with saponin, or with the membrane-permeable cross-linker DSP without cell permeabilization. Cell lysates were then immunoprecipitated with anti-RAP antibody and analyzed on SDS–PAGE under either non-reducing or reducing conditions. In each case, without the addition of cross-linker, no labeled protein was co-immunoprecipitated by the anti-RAP antibody. This indicates that the antibody does not cross-react with other cellular proteins. RAP itself is not labeled since its sequence lacks cysteine. With the addition of either cross-linker, labeled proteins can be seen. Under non-reducing conditions, labeled protein species migrated at the top of the gel, indicating that RAP has been cross-linked to other proteins which together migrated as large complexes. When the cross-linked materials were analyzed under reducing conditions, bands corresponding to the migration of LRP were seen with both cross-linkers. Since these experiments were performed with intact cells, they demonstrate directly an interaction between RAP and LRP within the cell. In order to confirm that the co-immunoprecipitation of LRP with RAP was due to their interaction as opposed to

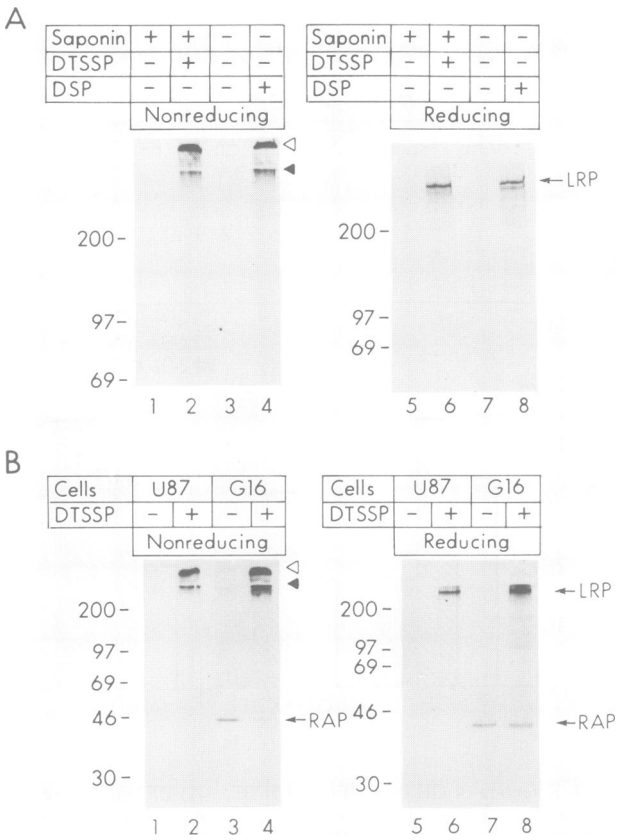

Fig. 5. Chemical cross-linking of LRP to RAP in U87 cells. (**A**) U87 cells were metabolically labeled with [^{35}S]cysteine for 5 h and incubated with PBSc in the absence or presence of cross-linkers. For membrane-impermeable cross-linker DTSSP, cells were first permeabilized with saponin, whereas they were cross-linked directly with membrane-permeable cross-linker DSP. Cell lysates were immunoprecipitated with anti-RAP antibody and were analyzed on 6% SDS–polyacrylamide gels under either non-reducing or reducing conditions. Open arrowhead indicates the top of the stacking gel, and the closed arrowhead refers to the top of the separating gel. The position of LRP is indicated with a closed arrow. RAP was not labeled in this experiment since it lacks cysteine in its sequence. (**B**) U87 cells and RAP stably transfected G16 cells were metabolically labeled with [^{35}S]methionine and [^{35}S]cysteine for 5 h, permeablized with saponin and incubated with PBSc either in the absence or presence of the cross-linker DTSSP. Cell lysates were immunoprecipitated with anti-RAP antibody and were analyzed on 10% SDS–polyacrylamide gels under either non-reducing or reducing conditions. The positions of LRP and RAP are indicated. Since U87 cells expresses lower amounts of RAP compared with the stably transfected G16 cells, the band corresponding to RAP is not visible for U87 cells at the above exposure, but is visible for G16 cells.

antibody cross-reactivity, we performed the same labeling, cross-linking and immunoprecipitation experiments in RAP-transfected G16 cells using both [^{35}S]cysteine and [^{35}S]methionine for labeling (Figure 5B). In comparison to U87 cells, RAP-transfected G16 cells exhibited a labeled band corresponding in size to that of RAP. Under non-reducing conditions, cross-linking with DTSSP decreased the intensity of RAP in G16 cells (compare lanes 3 and 4). Under reducing conditions, the cross-linked material generated both the LRP and RAP, confirming that both RAP and LRP were components of the cross-linked complexes. It is of note that LRP was the only major labeled protein cross-linked to RAP. We also performed DTSSP cross-linking with non-permeabilized U87 cells. No significant amount of LRP was cross-linked to RAP (data not shown), consistent with the fact that only a minimal amount of RAP (~2% of total) is present on the U87 cell surface (Bu *et al.*, 1994a).

Multiple regions of the 39 kDa protein can independently interact with LRP

In examining the RAP sequence for the presence of potential repeated domains, we noted a remarkable internal triplication (Figure 6A). When the RAP sequence is analyzed as three fragments of approximately equal size (amino acids 1–100, 101–200 and 201–323), we find identity between these regions ranging from 27% to as high as 40%. To investigate whether each of the three repeats from the human RAP sequence constitutes an independent domain capable of interacting with LRP, we generated overlapping cDNA constructs consisting of amino acids 1–110, 91–210 and 191–323, along with the full-length RAP cDNA (Figure 6B). These cDNA constructs were subcloned into the pGEX-2T expression vector to generate glutathione S-transferase (GST) fusion proteins in bacteria (Warshawsky *et al.*, 1993). The fusion proteins were purified to homogeneity and were recognized by both anti-GST and anti-RAP polyclonal antibodies on Western blots (data not shown). To examine whether each of these GST fusion proteins can interact with LRP, we performed ligand binding analysis with [^{35}S]cysteine-labeled U87 cells. Following binding at 4°C and washing, the remaining proteins were cross-linked to the U87 cell surface species using the membrane-impermeable cross-linker DTSSP (see above, Bu *et al.*, 1992). Cell lysates were then immunoprecipitated with anti-GST antibody and the resulting materials were analyzed by SDS–PAGE (Figure 6C). Without protein binding or following binding of GST alone, no LRP band was detected. However, with each of the three constructs, as well as with the full-length GST/RAP, LRP bands were seen, indicating that each of these species had interacted with and been cross-linked to LRP. The observation that each of the three internal triplicated domains may interact with LRP suggests that each RAP molecule is capable of interacting with more than one molecule of LRP. This may well contribute to the formation of the aggregated complexes discussed above (see Figure 5) which may include multiple RAP and LRP molecules.

Association of RAP with LRP is transient and coincides with the reduction of LRP ligand binding activity

To examine the kinetics of intracellular association of RAP and LRP and the effects of this association on LRP ligand binding activity, we performed pulse–chase experiments and examined the association of RAP with LRP kinetically. U87 cells were pulse-labeled with [^{35}S]cysteine for 30 min and chased for increasing periods of time up to 5 h. Cells were then permeablized with saponin to release soluble intracellular RAP. This procedure minimizes any additional association between RAP and LRP during cell lysis. Cell lysates were then prepared and divided into two parts. One portion from each chase period was immunoprecipitated with anti-RAP antibody in the absence of SDS (Figure 7A, top). Previous experiments had shown that LRP is co-immunoprecipitable with

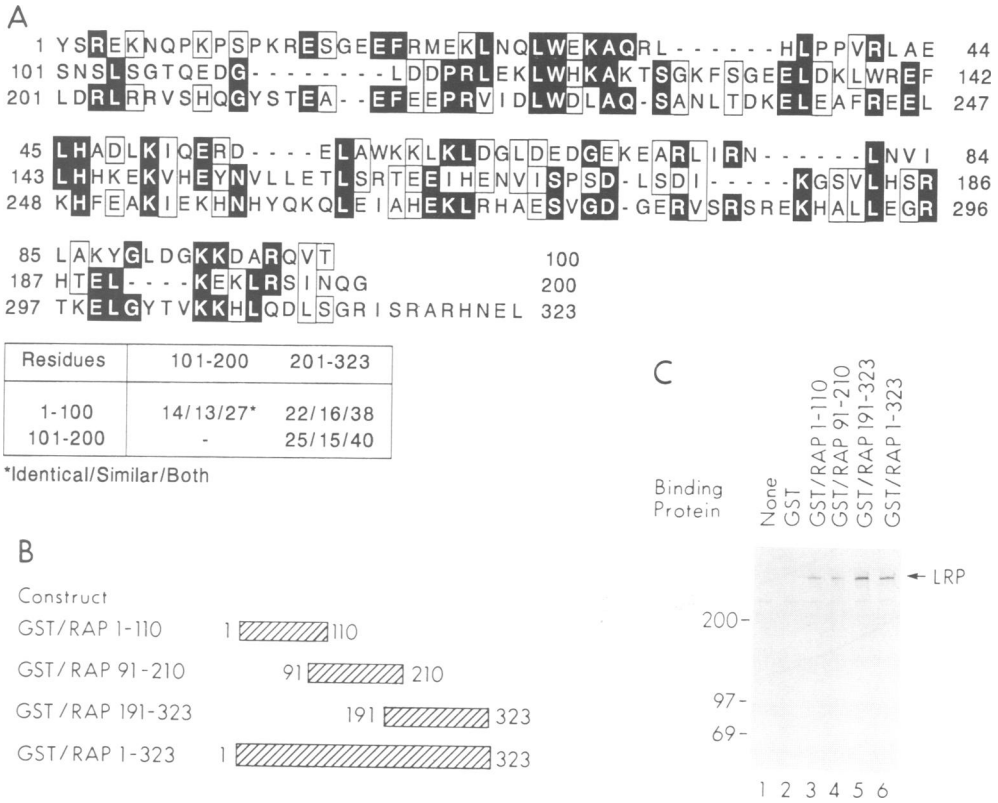

Fig. 6. RAP contains three internal triplicated domains, each can independently interact with LRP. (**A**) Amino acid sequence similarities among residues 1–100, 101–200 and 201–323 of RAP. Identical residues are on a closed box background, and conservative amino acid substitutions are on an open box background. The one-letter amino acid notation is used. (**B**) Schematic representation of GST/RAP constructs. All constructs were expressed as fusion proteins with GST and therefore contain GST at the N-termini. (**C**) U87 cells were metabolically labeled with [^{35}S]cysteine for 5 h. Binding with various GST/RAP constructs was then performed, followed with chemical cross-linking with DTSSP. Cells lysates were immunoprecipitated with anti-GST antibody and analyzed on 6% SDS–polyacrylamide gels under reducing conditions. The position of LRP is indicated.

RAP in the absence of SDS (also see Figure 8 below). The other portion was incubated with α_2M^*–Sepharose (Figure 7A, bottom), a well-established ligand for LRP (Bu *et al.*, 1992; Williams *et al.*, 1992; Warshawsky *et al.*, 1993). Radiolabeled LRP was extractable from the cell lysates by α_2M^*–Sepharose following longer chase times (Figure 7A). The intensity of each radiolabeled band was quantitated and plotted against the chase time (Figure 7B). As seen in the figure, the association of endogenous RAP with radiolabeled LRP reached a maximum early in the chase (0.5 h). The association gradually decreased to 40% of the maximum by 5 h of chase. In contrast, little α_2M^* binding activity of LRP was seen early in the chase period when RAP association was maximal. However, after ~2 h chase, α_2M^* binding activity increased to the maximum. This ligand binding activity of LRP decreased slightly following 2 h of chase and is probably a result of the cellular turnover of LRP molecules.

To examine whether changes in the ligand binding activity of LRP correlate with its dissociation from RAP, we performed the same pulse–chase labeling experiments as in Figure 7A, except that, after each chase period and cell permeabilization, intracellular proteins were cross-linked with DTSSP. When cell lysates were immunoprecipitated with anti-RAP antibody, the kinetics of LRP co-immunoprecipitation (data not shown) were similar to that observed in these non-cross-linked cells and shown in Figure 7A. However, when cell lysates were immunoprecipitated with anti-LRP antibody, the pattern of LRP seen on SDS–PAGE is intriguing (Figure 7C). Under non-reducing conditions, all cellular LRP in the early chase period (0–1 h) was cross-linked in large complexes migrating on the top of the gel. Since the cross-linking efficiency under these conditions was <40% (data not shown), each LRP molecule must have interacted with at least two RAP molecules in order for all of LRP to be cross-linked into RAP–LRP complexes. After ~1.5 h chase, free LRP was seen, indicating that some of the LRP molecules had dissociated from the RAP–LRP complexes. Although free LRP is apparent after 1.5 h chase, a substantial fraction of LRP remains associated with a high molecular weight complex, which may include RAP as well as other interacting proteins. These kinetic observations of free LRP generation following its *de novo* biosynthesis are similar to the kinetics of LRP ligand binding activity as seen in Figure 7A and B, and are consistent with the notion that RAP functions as a molecular chaperone by maintaining the receptor in a functionally inactive state early on in the secretory pathway. Under reducing conditions, the total amount of LRP remained similar at all chase periods, reflecting its relatively long half-life.

RAP dissociates from LRP under moderately low pH conditions of the Golgi

To examine whether the pH gradient along the secretory pathway contributes to the association/dissociation of

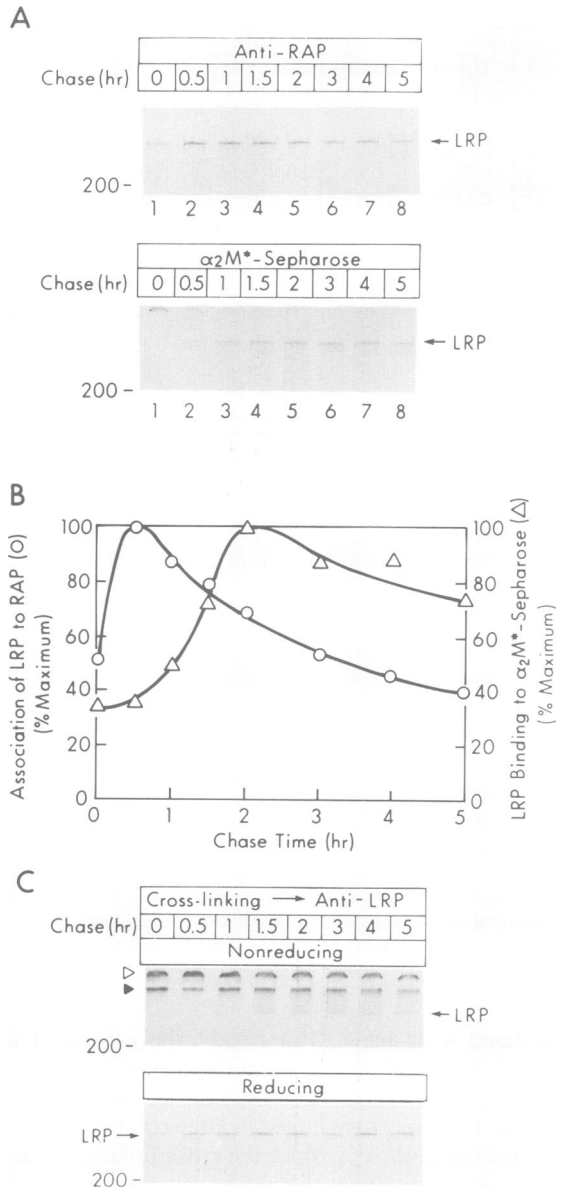

Fig. 7. Association of RAP with LRP inhibits LRP ligand binding activity. (**A**) U87 cells were pulse-labeled with [^{35}S]cysteine for 0.5 h and were chased for various periods of time as indicated. Cell lysates were either immunoprecipitated with anti-RAP antibody in the absence of SDS, or incubated with α_2M*–Sepharose beads. Samples were analyzed on 6% SDS–polyacrylamide gels under reducing conditions. The position of LRP is indicated. (**B**) The intensity of each band in (A) was measured by densitometry and plotted against the chase time. (**C**) U87 cells were pulse-labeled with [^{35}S]cysteine for 0.5 h and were chased for various periods of time as indicated. Cells were permeabilized with saponin and cross-linked with DTSSP. Cell lysates were then immunoprecipitated with anti-LRP antibody and were analyzed on 6% SDS–polyacrylamide gels under either non-reducing or reducing conditions. The position of LRP is indicated.

RAP and LRP, we analyzed RAP–LRP interactions under various pH conditions. U87 cells were metabolically labeled with [^{35}S]cysteine for 5 h following which cell lysates were immunoprecipitated under conditions of decreasing pH (Figure 8A). As in Figure 7A, LRP was co-immunoprecipitated with RAP at neutral pH (pH 7.2) in the absence of SDS (Figure 8A, lane 2). Anti-LRP antibody immunoprecipitated the same LRP band under identical pH conditions (lane 1). When Ca^{2+} was chelated in the immunoprecipitation mixture by EDTA, no LRP was co-immunoprecipitated with RAP, indicating that the interaction is calcium dependent (lane 3). LRP was also co-immunoprecipitated with RAP at pH 7.0 and 6.8 (lanes 4 and 5). However, at pH of 6.6 and below, LRP was no longer co-immunoprecipitated with RAP (lanes 6 and 7). This result was not due to a decreased interaction between RAP and the anti-RAP antibody at lower pH since the anti-RAP antibody immunoprecipitated [^{125}I]RAP identically under all pH conditions examined (Figure 8A, below). The pH-dependent dissociation may well be the determining factor for RAP dissociation from LRP *in vivo*. To confirm these results, we also performed [^{125}I]RAP binding to LRP on the U87 cell surface (Bu *et al.*, 1994a) under different pH conditions (Figure 8B). Maximum binding of [^{125}I]RAP to LRP was observed at pH 7.0. At pH of 6.6 and below, there is a dramatic decrease in [^{125}I]RAP binding. These results are consistent with those of the co-immunoprecipitation assays and strongly suggest a new type of mechanism by which a molecular chaperone departs from its target protein.

Discussion

Despite being widely used as a powerful tool in studying the biology of LRP, the physiological role of RAP is unknown. It is unlikely that the normal physiological function of RAP is extracellular since the protein has never been detected outside the cell. On the basis of the present results, we conclude that RAP is a molecular chaperone with LRP as its physiological target. Its function as a chaperone involves the regulation of LRP's ligand binding activity as the receptor travels through the secretory pathway. Via its interactions with LRP, RAP maintains LRP in a functionally inactive state until sorting to the cell surface. This appears to be physiologically important since all of the LRP ligands (e.g. t-PA, α_2M*, apoE) are secreted proteins and presumably travel by the same secretory pathway as LRP.

Although most of the molecular chaperones within the ER are involved in protein folding and the retention of unassembled proteins (Gething and Sambrook, 1992), recent evidence supports a role for molecular chaperones in the transport of substrate to a particular subcellular compartment as well as the controlled modulation of substrate activity (Hendrick and Hartl, 1993). Barks and Martens (1994) have recently demonstrated that the neuroendocrine polypeptide 7B2 belongs to this class of chaperones and functions by preventing the premature activation of the prohormone convertase PC2 within the secretory pathway. Similarly, the heat-shock protein 90 (hsp90) has been shown to regulate the glucocorticoid receptor activity (Pratt, 1993). We propose that RAP also belongs to this category of molecular chaperone. By maintaining LRP in an inactive and possibly aggregated state, RAP may effectively prevent other ligands from interacting with LRP prior to the time at which LRP matures to the cell surface. This function of RAP also resembles that of the invariant chain in regulating the peptide binding activity of MHC class II molecules (Sant and Miller, 1994). In the latter case, binding of the invariant chain to class II molecules prevents peptide

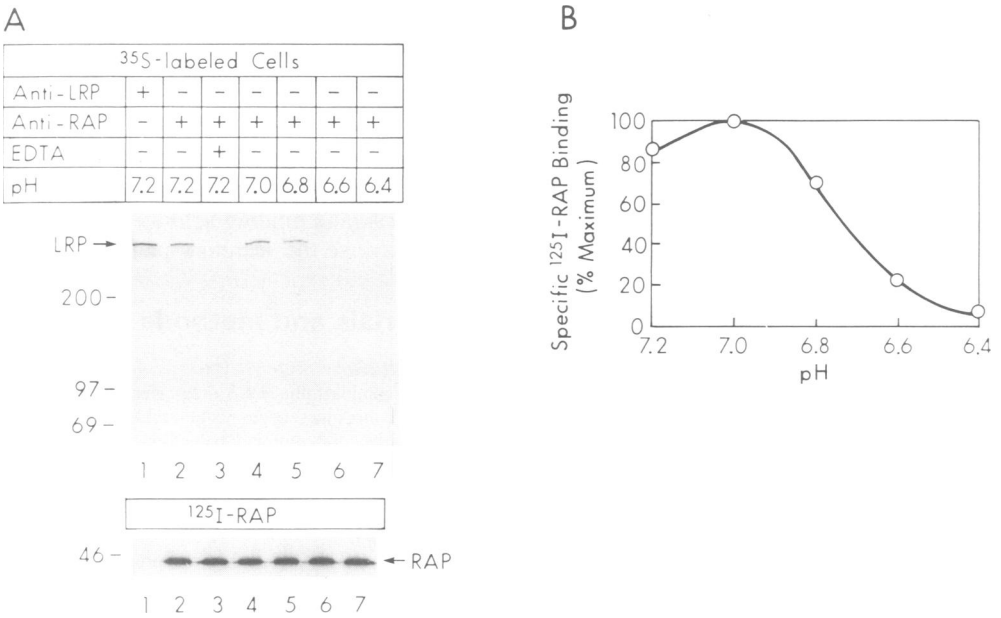

Fig. 8. pH-dependent dissociation of RAP from LRP. (**A**) U87 cells were metabolically labeled with [^{35}S]cysteine for 5 h. Cell lysates were immunoprecipitated with anti-RAP antibody with buffers of different pH as indicated. The immunoprecipitated materials were then analyzed on 6% SDS–polyacrylamide gels under reducing conditions. Below, [^{125}I]RAP were immunoprecipitated under the same conditions as for ^{35}S-labeled cell lysates. The positions of LRP and RAP are indicated. (**B**) Binding of [^{125}I]RAP was performed on U87 cells under different pH conditions. Specific binding for each pH was plotted against pH values. Each value represents the average of duplicate determinations and the standard deviations were <5%.

binding from taking place early in the biosynthesis and trafficking of the class II molecules.

The chaperone function of RAP requires the presence of this protein within the ER. Using several different experimental approaches, we demonstrate that the HNEL sequence at the C-terminus of RAP is both required for and sufficient to retain RAP within the ER. Although the HNEL sequence may resemble the well-known ER retention sequence KDEL (Munro and Pelham, 1987; Lewis and Pelham, 1990; Rothman and Orci, 1992), it probably represents a new mammalian ER retention sequence. Whether HNEL shares the same ER retention receptor with KDEL is not clear at present. However, it is possible that the two ER retention sequences may interact with the same receptor given the sequence similarity between the two signals. Since intracellular RAP lacks complex glycans added in the *trans*-Golgi (Kornfeld and Kornfeld, 1985), retrieval of RAP by the specific receptor must occur prior to exit from the medial-Golgi compartment.

The intracellular interaction between RAP and LRP was demonstrated not only by co-immunoprecipitation of LRP with RAP, but also via direct chemical cross-linking of the two proteins within intact cells. Previous studies suggesting an association between RAP and LRP have involved lysis of cells prior to co-immunoprecipitation of LRP with RAP (Strickland *et al.*, 1991). However, the possibility exists that association of the two proteins occurred as a result of the disorganization of intracellular compartments during cell lysis. By use of a membrane-permeable chemical cross-linking reagent, we demonstrated the association of the two proteins prior to cell lysis. It is interesting to note that when cells were permeabilized with the permeabilization reagent saponin, ~60% of the total intracellular RAP was released (data not shown), indicating that this portion of RAP was not associated with a membrane-bound protein. It is possible that these soluble RAP molecules interact with other resident proteins within the ER. In fact, following cross-linking with DSP in U87 cells labeled with [^{35}S]-methionine, we observed several proteins of variable sizes that were cross-linked to RAP (data not shown).

The mechanism by which RAP associates with LRP within cells is not entirely clear. However, our cross-linking experiments suggest the formation of large aggregates which contain both RAP and LRP. The internal triplication within the RAP sequence results in three independent functional domains, each of which can interact with LRP. Within LRP molecules, there are also multiple RAP binding domains. For example, using a truncated LRP minireceptor system, Willnow *et al.* (1994) have recently demonstrated that there were at least two independent RAP binding domains on LRP. Therefore, both multiple LRP binding domains on RAP and multiple RAP binding domains on LRP may contribute to the formation of RAP–LRP aggregates. Alternatively, RAP binding to LRP may induce a conformational change in LRP such that LRP molecules migrate toward one another to form aggregates. Either a conformational change in LRP or aggregation itself may be responsible for LRP inactivation.

The kinetics of the association of RAP and LRP demonstrated that this association decreased as LRP migrated through the secretory pathway and correlated with an increase in LRP ligand binding activity. More intriguingly, RAP dissociation from LRP occurs at a pH of 6.6 or below. Since the pH within the Golgi compartment is ~6.4–6.6 (Chanat and Huttner, 1991), it appears likely that *in vivo* RAP dissociates from LRP within the Golgi. The fact that intracellular RAP lacks complex carbohydrate modification, which is normally added in the *trans*-

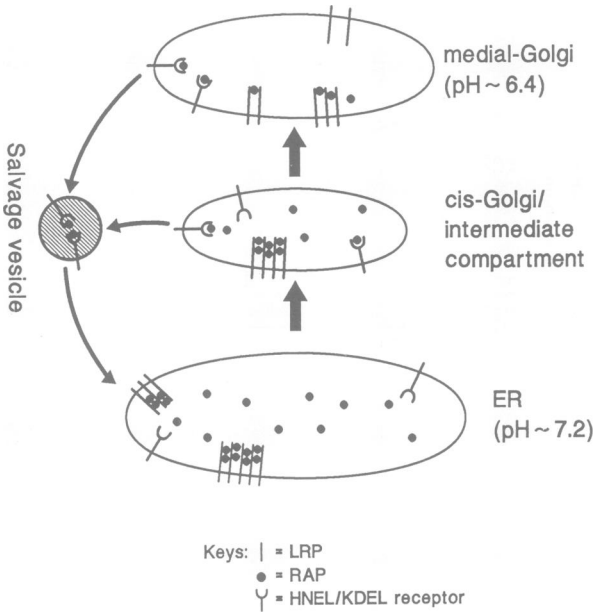

Fig. 9. Model of intracellular RAP function as a molecular chaperone for RAP. Inside the ER, RAP exists both in soluble form and in aggregation with multiple LRP molecules. The association of RAP with LRP keeps LRP in a functionally inactive state. RAP–LRP aggregates travel together to the medial-Golgi compartment where they dissociate from each other as a result of lower pH. LRP proceeds to the cell surface in a functionally active state, while RAP molecules are retrieved back to the ER by HNEL/KDEL receptors where they continue their chaperone functions.

Golgi compartment (Kornfeld and Kornfeld, 1985), further suggests that the dissociation between RAP and LRP takes place in the medial-Golgi compartment. It is possible that other factors such as calcium concentration may also contribute to the association/dissociation of LRP and RAP. However, the pH drop along the secretory pathway alone would be sufficient to promote the dissociation of RAP from LRP. Based upon our current results, a model depicting the molecular chaperone function of RAP is proposed (Figure 9). In this model, the majority of RAP resides within the ER. Soon after the biosynthesis of LRP, RAP associates with the receptor and initiates the formation of multi-molecular aggregates. Within these aggregates LRP is inactive in ligand binding. Following their trafficking together to the medial-Golgi compartment, RAP dissociates from LRP as a result of the low pH. The dissociated RAP may exhibit a high affinity for the retrieval receptor at low pH, similar to that seen with the KDEL/KDEL receptor system *in vitro* (Wilson *et al.*, 1993). The retrieval receptors shuttle RAP back to the ER where neutral pH unloads RAP from its retrieval receptor. These RAP molecules may then interact with additional LRP molecules to reinitiate their chaperone function. The low pH within the medial- and *trans*-Golgi which facilitates RAP dissociation also impedes the binding of other LRP ligands to LRP within the terminal portions of the secretory pathway (Maxfield and Yamashiro, 1991). This facilitates the coordinate secretion of LRP ligands (e.g. α_2M^*, t-PA, apoE) and delivery of unliganded LRP to the cell surface.

While only experiments performed with U87 cells are shown in the present study, many of the key experiments (e.g. intracellular cross-linking between LRP and RAP) have also been performed with other cell types including human hepatoma HepG2 cells and rat hepatoma MH_1C_1 cells (Bu *et al.*, 1992, 1993; data not shown) and yield identical results. Therefore, the molecular chaperone function of RAP for LRP appears to be a general function of RAP in all cells which express LRP. Furthermore, it is also possible that other cellular receptors are also regulated in their ligand binding activity via similar mechanisms as they traverse the secretory pathway.

Materials and methods

Cell culture

Human glioblastoma U87 cells were cultured in Earle's minimum essential medium supplemented with 10% fetal calf serum, 2 mM L-glutamine, 100 units/ml penicillin, 100 μg/ml streptomycin, 1 mM sodium pyruvate, and maintained at 37°C in humidified air containing 5% CO_2 as described previously (Bu *et al.*, 1994a).

Antibodies

Polyclonal anti-RAP antibody was prepared in rabbits against recombinant human RAP (Bu *et al.*, 1994a). Specific anti-RAP IgG was purified with a RAP–Sepharose column after total anti-RAP IgG was prepared with protein A–agarose. Polyclonal anti-LRP antiserum, anti-GH antiserum and anti-GST antiserum were generated in rabbits using human LRP purified from human placenta, recombinant human GH and recombinant GST protein, respectively.

PCR cloning of cDNAs and plasmid construction

Human full-length RAP and RAPΔHNEL cDNAs were prepared using RT-PCR techniques as described before (Bu *et al.*, 1994b). Briefly, mRNA from U87 cells and random primers were used for RT reaction to generate first strand cDNAs. The RT reaction mixtures were then used for the PCR using the following primers: for full-length RAP, 5′ primer GATCGGATCCGGGATGATGGCGCCGCGGAGGGTCA, 3′ primer GATCCTCGAGTCAGAGTTCGTTGTGCCGAGCTC; for RAPΔHNEL, 5′ primers was identical to that for the full-length RAP, and the 3′ primer was GATCCTCGAGTCACCGAGCTCTGGAGATCCTGCCG. The 5′ primer contained a built-in *Bam*HI site, whereas each of the 3′ primers included a built-in *Xho*I site. The PCR reactions were cycled once for 5 min at 95°C before *Taq* DNA polymerase was added. This was followed with 30 cycles of 30 s at 60°C, 2 min at 72°C and 30 s at 95°C. The resulting PCR products were digested with *Bam*HI and *Xho*I and subcloned into the pcDNA3 expression vector (Invitrogen). For the three GH constructs, each cDNA was generated using full-length human GH cDNA (generously provided by Genentech) as the template. The common 5′ primer was GATCAAGCTTCTGCAATGGCTACAGGCTCCCG (with a built-in *Hin*dIII site). The three 3′ primers were: for wild-type GH: GATCGGATCCCTAGAAGCCACAGCTGCCCTCC; for GH+KDEL: GATCGGATCCCTAGAGTTCATCTTTGAAGCCACAGCTGCCCTCCACA; and for GH+HNEL: GATCGGATCCCTAGAGTTCGTTGTGGAAGCCACAGCTGCCTCCACA. Each of the 3′ primers contained a built-in *Bam*HI site. The PCR was carried out essentially as described above except the elongation period was 1 min. The three PCR products were then digested with *Hin*dIII and *Bam*HI before they were subcloned into pcDNA3. The pGEX–RAP constructs were prepared using PCR essentially as described before (Warshawsky *et al.*, 1993) except human RAP cDNA in pcDNA3 was used as the template. For each construct the primers are listed below: GST/RAP1–110: 5′ primer, GATCGGATCCTACTCGCGGGAGAAGAACCAGCC, 3′ primer, GATCGAATTCTCAGTCTTCCTGGGTGCCACTGAGGG; GST/RAP91–210: 5′ primer, GATCGGATCCGACGGAAAGAAGGACGCTCGGCAG, 3′ primer, GATCGAATTCTCACTGGTGGCTGACCCTGCGCAGGC; GST/RAP191–323: 5′ primer, GATCGGATCCAAGGAGAAGCTGCGCAGCATCAAC, 3′ primer, GATCGAATTCTCAGAGTTCGTTGTGCCGAGCTC; and GST/RAP1–323, 5′ primer was the same as the 5′ primer for GST/RAP1–100, and 3′ primer was the same as the 3′ primer for GST/RAP191–323. All the cDNA sequences generated by RT-PCR or PCR were verified by sequencing.

Transient and stable transfections

U87 cells were transfected with various plasmids at ~50% confluence using Lipofectin reagent (BRL). For 10 cm dishes of U87 cells, 10 μg DNA and 50 μl Lipofectin in serum-free medium were used. Serum-

containing medium was added after 5 h of transfection. Cells were trypsinized after 48 h of transfection. For transient transfection, cells were replated in smaller sized dishes or multi-well plates and assayed the next day. For stable transfection, cells were plated to low densities in medium containing G418 (0.4 mg/ml). Individual colonies were then selected and assayed for the target protein by Western blotting. Positive clones were grown as individual cell lines. Generally, five clones for each transfection were established before a representative one was used for further analysis.

Metabolic labeling and pulse–chase experiments

For continuous metabolic labeling, cells at ~80% confluence were incubated for 30 min at 37°C with two changes of serum-free medium lacking either methionine, or cysteine or both. Metabolic labeling was initiated by the addition of the above medium supplemented with the corresponding [^{35}S]methionine, or [^{35}S]cysteine or both (200 μCi/ml). The labeling was continuous for various periods of time as specified in each experiment. For pulse–chase experiments, cells were pulse-labeled with either [^{35}S]methionine or [^{35}S]cysteine for 30 min, and chased with serum-containing medium for different periods of time, as specified in each experiment. The total amount of labeled protein for each chase period was normalized by applying equal amounts of TCA-precipitable radioactivity for immunoprecipitation.

Immunoelectron microscopy

G16 and H1 cells were fixed in a mixture of 2% paraformaldehyde and 1% acrolein in 0.1 M sodium phosphate buffer, pH 7.4, for 2 h and kept in 1% paraformaldehyde in the same buffer until further processing. Cell samples were embedded in 10% gelatin which was solidified on ice. Blocks with cells were immersed in 2.3 M sucrose in phosphate buffer prior to cryosectioning. Ultra-thin cryosections were picked up from the knife and were immunolabeled with 10 nm protein A-conjugated colloid gold probes (Slot and Geuze, 1985). The labeled sections were contrasted and embedded as described previously (Slot *et al.*, 1988).

Chemical cross-linking

Cells were washed three times on ice with pre-chilled phosphate-buffered saline (PBS) supplemented with 1 mM $CaCl_2$ and 0.5 mM $MgCl_2$ (PBSc). For intracellular cross-linking with DTSSP, cells were first permeablized with 0.1% saponin (w/v) for 30 min at 4°C. DTSSP (0.5 mM final) in PBSc was added and cells were cross-linked for 30 min at 4°C. For cross-linking with DSP, a stock solution (50 mM) was prepared in dimethylsulfoxide (DMSO) and added to PBSc on the cells (final concentration was 1 mM). The cross-linking reaction was carried out at 4°C for 30 min. All the cross-linking reactions were quenched by washing cell monolayers three times with Tris-buffered saline (TBS). Cells were then lysed in PBSc containing 1% (v/v) Triton X-100 and 1 mM phenylmethylsulfonylfluoride (PMSF) and used for immunoprecipitation as described below.

Immunoprecipitations and SDS–PAGE

Immunoprecipitations were carried out essentially as described before (Bu *et al.*, 1993). For immunoprecipitation in the absence of SDS, the washing solution was PBSc containing 0.5% (v/v) Triton X-100 and 1 mM PMSF. Primary antibodies used for 1 ml of immunoprecipitation were 4 μg specific anti-RAP IgG, 10 μl anti-LRP serum, 10 μl anti-GH serum or 10 μl anti-GST serum. The immunoprecipitated materials were released from the beads by boiling each sample for 5 min in SDS sample buffer [62.5 mM Tris–HCl, pH 6.8, 2% (w/v) SDS, 10% (v/v) glycerol] (Laemmli, 1970). For samples analyzed under reducing conditions, 5% (v/v) β-mercaptoethanol was included in the SDS sample buffer. The percentage of SDS–polyacrylamide gels is indicated in each figure legend. Rainbow molecular weight markers (BioRad) were used as the molecular weight standards.

Endo H digestion

After immunoprecipitation, protein A beads were boiled in 100 mM sodium acetate, pH 5.5, containing 0.4% SDS. Each elution was divided into two equal parts. The control portion was combined with an equal volume of 100 mM sodium acetate, pH 5.5, without endo H. The experimental portion was added to an equal volume of the same buffer containing 1 mU of endo H (Boehringer Mannheim). The digestion was carried out at 37°C for 16 h before the samples were analyzed via SDS–PAGE.

pH-dependent association of LRP with RAP

Each pH buffer consisted of 50 mM buffer reagent and 150 mM NaCl. For pH 6.8–7.2, *N*-2-hydroxyethylpiperazine-*N'*-2-ethanesulfonic acid (HEPES) was used as the buffer reagent, whereas 2-(4-morpholino)-ethane sulfonic acid (MES) was used for pH 6.4–6.6. For co-immunoprecipitation experiments, [^{35}S]cysteine-labeled U87 cells were lysed in 10 mM HEPES buffer, pH 7.2, containing 150 mM NaCl, 1% (v/v) Triton X-100 and 1 mM PMSF. A 100 μl aliquot of the ^{35}S-labeled cell lysate was mixed with 900 μl of each pH buffer for immunoprecipitation. Protein A beads were washed three times with the corresponding pH buffer containing 0.5% (v/v) Triton X-100 and three times with PBSc before proteins were eluted and analyzed. For the [^{125}I]RAP ligand binding experiment (Bu *et al.*, 1994b), cell monolayers were washed twice with PBSc and twice with the pH buffer. Ligand binding was carried out in the corresponding pH buffer in the absence or presence of unlabeled ligand.

Ligand binding and cross-linking of GST/RAP constructs

Production and purification of the recombinant GST/RAP proteins expressed in bacteria have been described previously (Williams *et al.*, 1992; Bu *et al.*, 1993). Cells were metabolically labeled with [^{35}S]-cysteine, as described before. Ligand binding assays were carried out by incubating each ligand (10 nM) in PBSc with the cells for 1 h at 4°C. Unbound ligands were washed away before cell surface cross-linking with DTSSP was performed. Each cell lysate was immunoprecipitated with anti-GST antiserum as described above.

Acknowledgements

We wish to thank Stephanie Rennke for purifying GST/RAP fusion proteins, Janice Griffiths for expert assistance with immunoelectron microscopy. We are also indebted to Stuard Kornfeld, Jonathan Gitlin and David Wilson for critical reading of the manuscript. This work was supported by grants from the NIH (HL52040, HL53280, AG05681) to A.L.S. and G.B., and the Netherlands Organization for Scientific Research (NWO) to H.J.G.

References

Barks,J.A. and Martens,G.J. (1994) *Cell*, **78**, 263–273.
Beisiegel,U., Weber,W., Ihrke,G., Herz,J. and Stanley,K.K. (1989) *Nature*, **341**, 162–164.
Bu,G., Williams,S., Strickland,D.K. and Schwartz,A.L. (1992) *Proc. Natl Acad. Sci. USA*, **89**, 7427–7431.
Bu,G., Maksymovitch,E.A. and Schwartz,A.L. (1993) *J. Biol. Chem.*, **268**, 13002–13009.
Bu,G., Maksymovitch,E.A., Geuze,H. and Schwartz,A.L. (1994a) *J. Biol. Chem.*, **269**, 29874–29882.
Bu,G., Maksymovitch,E.A., Nerbonne,J.M. and Schwartz,A.L. (1994b) *J. Biol. Chem.*, **269**, 18521–18528.
Chanat,E. and Huttner,W.B. (1991) *J. Cell Biol.*, **115**, 1505–1519.
Gething,M.-J. and Sambrook,J. (1992) *Nature*, **355**, 33–45.
Hendrick,J.P. and Hartl,F.-U. (1993) *Annu. Rev. Biochem.*, **62**, 349–384.
Herz,J., Hamann,U., Rogne,S.K., Myklebost,O., Gausepohl,H. and Stanley,K.K. (1988) *EMBO J.*, **7**, 4119–4127.
Herz,J., Goldstein,J.L., Strickland,D.K., Ho,Y.K. and Brown,M.S. (1991) *J. Biol. Chem.*, **266**, 21232–21238.
Herz,J., Clouthier,D.E. and Hammer,R.E. (1992) *Cell*, **71**, 411–421.
Iadonato,S.P., Bu,G., Maksymovitch,E.A. and Schwartz,A.L. (1993) *Biochem. J.*, **296**, 867- 875.
Kornfeld,R. and Kornfeld,S. (1985) *Annu. Rev. Biochem.*, **54**, 631–664.
Kounnas,M.Z., Morris,R.E., Thompson,M.R., Fitzgerald,D.J., Strickland, D.K. and Saelinger,C.B. (1992) *J. Biol. Chem.*, **267**, 12420–12423.
Kowal,R.C., Herz,J., Goldstein,J.L., Esser,V. and Brown,M.S. (1989) *Proc. Natl Acad. Sci. USA*, **86**, 5810–5814.
Krieger,M. and Herz,J. (1994) *Annu. Rev. Biochem.*, **63**, 601–637.
Kristensen,T., Moestrup,S.K., Gliemann,J., Bendtsen,L., Sand,O. and Sottrup-Jensen,L. (1990) *FEBS Lett.*, **276**, 151–155.
Laemmli,U.K. (1970) *Nature*, **227**, 680–685.
Lewis,M.J. and Pelham,H.R. (1990) Nature, **348**, 162–163.
Maxfield,F.R. and Yamashiro,D.J. (1991) In Steer,C.J. and Hanover,J.A. (eds), *Intracellular Trafficking of Proteins.* Cambridge University Press, Cambridge, pp. 157–182.
Munro,S. and Pelham,H.R. (1987) *Cell*, **48**, 899–907.
Nykjaer,A., Petersen,C.M., Moller,B., Jensen,P., Moestrup,S.K., Holtet,T., Etzerodt,M., Thogersen,H.C., Munch,M., Andreasen,P.A. and Gliemann,J. (1992) *J. Biol. Chem.*, **267**, 14543–14546.
Orth,K., Madison,E.L., Gething,M-J., Sambrook,J.F. and Herz,J. (1992) *Proc. Natl Acad. Sci. USA*, **89**, 7422–7426.

Pietromonaco,S., Kerjaschki,D., Binder,S., Ullrich,R. and Farquhar,M.G. (1990) *Proc. Natl Acad. Sci. USA*, **87**, 1811–1815.
Pratt,W.B. (1993) *J. Biol. Chem.*, **268**, 21455–21458.
Raychowdhury,R., Niles,J.L., McCluskey,R.T. and Smith,J.A. (1989) *Science*, **244**, 1163–1165.
Rothman,J.E. and Orci,L. (1992) *Nature*, **355**, 409–415.
Sant,A.J. and Miller,J. (1994) *Curr. Opin. Immunol.*, **6**, 57–63.
Schwaninger,R., Beckers,C.J.M. and Balch,W.E. (1991) *J. Biol. Chem.*, **266**, 13055–13063.
Schweizer,A., Fransen,J.A.M., Bachi,T., Ginsel,L. and Hauri,H. (1988) *J. Cell Biol.*, **107**, 1643–1653.
Slot,J.W. and Geuze,H.J. (1985) *Eur. J. Cell Biol.*, **38**, 87–93.
Slot,J.W., Weerkamp,A.H. and Geuze,H.J. (1988) *Methods Microbiol.*, **20**, 211–236.
Strickland,D.K., Ashcom,J.D., Williams,S., Burgess,W.H., Migliorini,M. and Argraves,W.S. (1990) *J. Biol. Chem.*, **265**, 17401–17404.
Strickland,D.K., Ashcom,J.D., Williams,S., Battey,F., Behre,E., McTigue,K., Battey,J.F. and Argraves,W.S. (1991) *J. Biol. Chem.*, **266**, 13364–13369.
Takakashi,S., Kawarabayasi,Y., Nakai,T., Sakai,J. and Yamamoto,T. (1992) *Proc. Natl Acad. Sci. USA*, **89**, 9252–9256.
Warshawsky,I., Bu,G. and Schwartz,A.L. (1993) *J. Biol. Chem.*, **268**, 22046–22054.
Warshawsky,I., Broze,G.J.Jr and Schwartz,A.L. (1994) *Proc. Natl Acad. Sci. USA*, **91**, 6664–6668.
Williams,S.E., Ashcom,J.D., Argraves,W.S. and Strickland,D.K. (1992) *J. Biol. Chem.*, **267**, 9035–9040.
Willnow,T.E., Goldstein,J.L., Orth,K., Brown,M.S. and Herz,J. (1992) *J. Biol. Chem.*, **267**, 26172–26180.
Willnow,T.E., Orth,K. and Herz,J. (1994) *J. Biol. Chem.*, **269**, 15827–15832.
Wilson,D.W., Lewis,M.J. and Pelham,H.R. (1993) *J. Biol. Chem.*, **268**, 7465–7468.
Yamamoto,T., Davis,G.C., Brown,M.S., Schneider,W.J., Casey,M.L., Goldstein,J.L. and Russel,D.W. (1984) *Cell*, **39**, 27–38.

Received on January 16, 1995; revised on February 14, 1995